

In-plane paraconductivity in a single crystal of superconducting $\text{YBa}_2\text{Cu}_3\text{O}_{7-x}$

T. A. Friedmann, J. P. Rice, John Giapintzakis, and D. M. Ginsberg

*Department of Physics and Materials Research Laboratory, University of Illinois at Urbana-Champaign,
1110 West Green Street, Urbana, Illinois 61801*

(Received 16 November 1988)

Resistivity measurements have been made in the a - b plane on a single-crystal sample of superconducting $\text{YBa}_2\text{Cu}_3\text{O}_{7-x}$. The resistivity versus temperature curve shows a highly linear region between 150 and 240 K, with an upward deviation from linearity at 240 K. With decreasing temperature below 150 K, the resistivity curve also deviates from linearity; this deviation has been analyzed in terms of the Aslamazov-Larkin, Lawrence-Doniach, and Maki-Thompson paraconductivity theories. All three theories can be fit to the data, but the Lawrence-Doniach model gives the best fit to the data, with physically reasonable parameters. We find that the Ginzburg-Landau coherence length in the c direction, extrapolated to low temperature with the theoretical temperature dependence, is approximately 0.44 Å.

I. INTRODUCTION

We have made resistivity measurements in the a - b plane on a single crystal of $\text{YBa}_2\text{Cu}_3\text{O}_{7-x}$ and have analyzed the data to determine how the conductivity is affected by fluctuations of small regions of the sample into the superconducting state. The part of the conductivity caused by these fluctuations is called the paraconductivity. It is usually too small to measure in conventional superconductors, although it can be seen if the electron mean free path and, hence, the coherence length is small enough. Paraconductivity was first seen in amorphous bismuth.¹

The nature of the in-plane paraconductivity in $\text{YBa}_2\text{Cu}_3\text{O}_{7-x}$ has been a matter of some debate. Initial measurements on polycrystalline samples by several groups²⁻⁴ were fit to the three-dimensional Aslamazov-Larkin (3D AL) model.⁵ Their fits to the data indicated general agreement with the model up to a reduced temperature $\epsilon = (T - T_c^{\text{MF}})/T_c^{\text{MF}} = 0.1$ with an effective coherence length ranging between 13 and 22 Å. (T_c^{MF} is the mean-field transition temperature.) Above $\epsilon = 0.1$ the paraconductivity fell rapidly to zero in those studies.

Oh *et al.*⁶ made measurements on highly c -axis-oriented thin films which they analyzed in terms of the Lawrence-Doniach⁷ (LD) model. Their analysis indicated a temperature dependence in qualitative agreement with the LD theory over a range $0.005 < \epsilon < 0.5$. The magnitude of the paraconductivity, however, was only 0.14 to 0.3 times that predicted by the LD theory, and the mean-field transition temperature was 1–2 K above the zero-resistance value T_c .

Measurements by Hagen, Wang, and Ong⁸ on single-crystal $\text{YBa}_2\text{Cu}_3\text{O}_{7-x}$ samples were analyzed in terms of the two-dimensional AL theory (2D AL). Their results indicated a good fit to the data over a wide range, $0.06 < \epsilon < 1.9$. The fits indicated a mean-field transition temperature 3–5 K below T_c . The thickness of the model's 2D superconducting layer d ranged from 5.7 to 30 Å and was uncorrelated with the transition width ΔT_c and the room-temperature resistivity. Hagen *et al.* concluded

that their data did not fit the LD model.

In this paper we describe data obtained for a single-crystal sample of $\text{YBa}_2\text{Cu}_3\text{O}_{7-x}$ having an extremely linear dependence on temperatures between 150 and 240 K. We compare our data with predictions of the Aslamazov-Larkin, Maki-Thompson,^{9,10} and Lawrence-Doniach theories.

II. EXPERIMENTAL METHOD

The crystal explored in this study was grown by a self-flux method employing an excess of copper oxide, as described elsewhere.¹¹ It was twinned, like almost all crystals of $\text{YBa}_2\text{Cu}_3\text{O}_{7-x}$. The dimensions of the sample were $2.0 \times 0.62 \times 0.016$ mm³. (The c direction was the shortest dimension.) To provide electrical contact to the sample, four strips of gold, 1 μm in thickness and 0.025 mm wide, were evaporated through a mask onto the surface in a standard four-probe configuration, producing the electrodes shown in Fig. 1. (The van der Pauw configuration¹² was not used because the sample was very thin and would have fractured in putting electrodes on its corners.) The gold strips were fixed to the sample by heating it in flowing O_2 for 1 h at 600°C, oven cooling it to 400°C, and finally quenching it to room temperature in

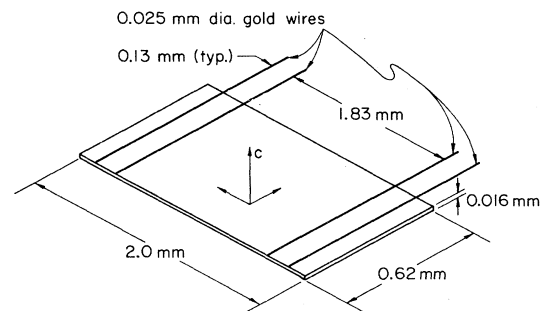


FIG. 1. Sample dimensions and contact geometry.

air from 400 °C. Ultrasonic bonding of gold wires, 0.025 mm in diameter, to the gold strips was followed by a heat treatment performed in flowing O₂ at 600 °C for 1 h, an oven cooling to 400 °C, and a soak of 60 h at this temperature. The sample was then quench cooled in air. The resulting contact resistances were less than 1 Ω.

Using GE 7031 varnish, the sample was mounted on a sapphire substrate which was varnished to a copper block. The resistance was measured with an ac bridge¹³ at a frequency of 95 Hz. The sensitivity of the bridge was 10⁻⁵ Ω. The temperature, measured with a calibrated carbon glass thermometer, was stabilized to within ±1 mK for 90 < T < 125 K and within ±10 mK for 125 < T < 300 K. The resistive transition was measured at two different current densities, 7.5 A/cm² and 0.75 A/cm², with the results having a negligible dependence on current density. The data taken with the larger current density are reported in this paper.

III. RESULTS

A. General features

Magnetization measurements (Fig. 2) were carried out in a superconducting quantum interference-based magnetometer in a field $H = 14$ Oe applied perpendicular to the crystal's c axis. The transition had a width (10% to 90% of the transition) of 3 K and a midpoint of 89 K. The zero-field-cooled shielding fraction (uncorrected for "demagnetization") was 82%, and the field-cooled Meissner fraction (also uncorrected) was 41% of the ideal value $1/4\pi$. Flux pinning makes this a lower limit on the frac-

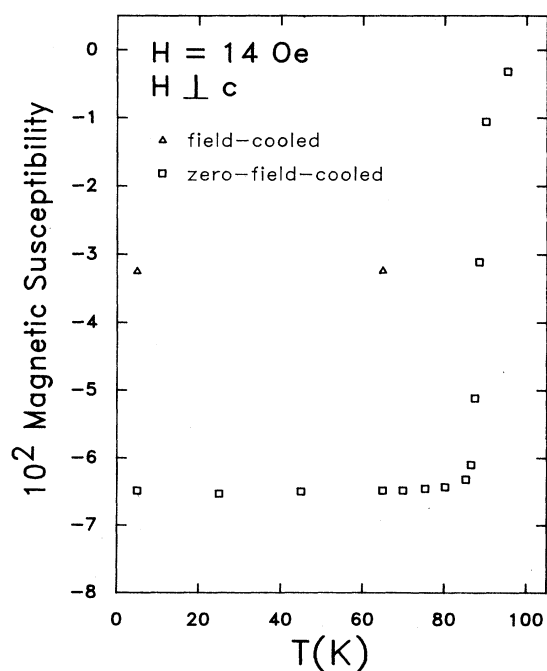


FIG. 2. Magnetic susceptibility (in Gaussian units) vs T zero-field-cooled (ZFC) and field cooled (FC).

tion of the sample, which was superconducting.

The room-temperature resistivity was $\rho(295) = 222 \pm 44 \mu\Omega \text{ cm}$. The zero-resistance transition temperature was $T_c = 93.0$ K. A plot of the derivative $d\rho/dT$ vs T (Fig. 3) indicates a narrow transition (full width at half-maximum = 0.37 K) with some structure at the peak of the curve, suggesting two closely spaced superconducting transitions. (Note: Hagen *et al.* report narrow transitions with no structure in the $d\rho/dT$ curves, but their data were not as closely spaced in temperature, so they would not have seen the small structure reported here if it were present in their samples.)

At higher temperatures, the $d\rho/dT$ curve (Fig. 4) indicates a region 90 K wide, from 150 to 240 K, which is very nearly linear. A fit to the data over this region to $\rho = aT + b$ gives a slope $a = 0.724 \mu\Omega \text{ cm/K}$ and an intercept $b = 2.84 \mu\Omega \text{ cm}$. The extreme linearity of ρ in this region, for which a theoretical reason has been suggested,¹⁴ provides us with a basis for carefully studying the non-linear region below 150 K. The deviation of the curve from linearity above 240 K may be associated with other indications of anomalous behavior around 240 K.^{15,16}

B. Fitting procedure

The data were fit to four theoretical models (2D AL, 3D AL, LD, and MT) by using a Levenberg-Marquardt-based nonlinear least-squares fitting routine.¹⁷ The measured conductivity is taken to be

$$\sigma = \sigma_n + \sigma', \quad (1)$$

where σ_n represents the normal-state conductivity and σ' the paraconductivity contribution. In all cases, we as-

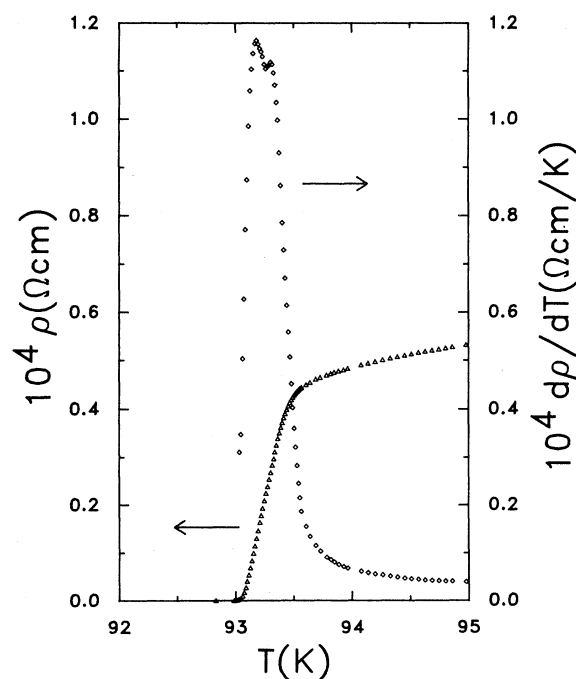
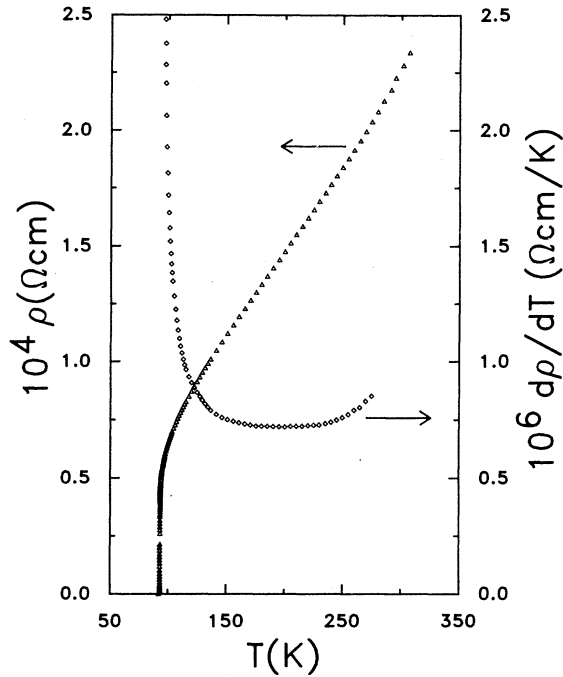


FIG. 3. ρ vs T and $d\rho/dT$ vs T near the transition temperature.

FIG. 4. ρ vs T and $d\rho/dT$ vs T .

sumed the normal-state conductivity to be

$$\sigma_n = 1/(aT + b), \quad (2)$$

corresponding to a linear resistivity. The functional form of σ' to which we have fit the data depends on the theoretical model used. The data were fit to temperature values greater than $2T_c$. The reduced temperature $\epsilon = (T - T_c^{\text{MF}})/T_c^{\text{MF}}$ is, for small ϵ , the first term in the expansion of $\ln(T/T_c^{\text{MF}})$.¹⁸ Since this approximation is not valid at temperatures all the way up to $2T_c$, we replaced ϵ with $\epsilon_l = \ln(T/T_c^{\text{MF}})$ in the equations usually used to fit paraconductivity data.

The best fit to the data is defined to be the one which minimizes

$$\chi^2 = \sum_{n=1}^N [\sigma_{\text{fit}}(T_n) - \sigma(T_n)]^2 / (N - P), \quad (3)$$

where N is the number of data points and P is the number of fitting parameters. In the 2D AL and 3D AL models $P=4$, and in the MT and LD models $P=5$. With so many fitting parameters, it is possible that the fitting pro-

cedure could end up in a minimum of χ^2 that was local but not global. To ensure that the fitting routine had found the lowest minima in χ^2 , a grid procedure was followed for all of the fits reported below. This procedure starts the Levenberg-Marquardt fitting routine at many initial values for the parameters (including a and b) throughout the range of physically reasonable values. In each case, over one hundred initial parameter settings were attempted in order to approach the minimum in χ^2 from different directions in the parameter space. In addition, the best fits for each model were confirmed by using a simulated annealing technique.¹⁹ This technique gave the same results as the Levenberg-Marquardt method with our grid procedure. The χ^2 values reported below have all been normalized to the χ^2 value for the fit labeled AL2a in Table I.

C. Fit to the AL model

The AL model takes into account the electric field's acceleration of the short-lived superconducting pairs which form above T_c . The functional form of the paraconductivity depends on the dimensionality of the superconductivity

$$\sigma' = \frac{e^2}{16\hbar d} \epsilon_l^{-1} \quad (2D), \quad (4)$$

$$\sigma' = \frac{e^2}{32\hbar \xi(0)} \epsilon_l^{-1/2} \quad (3D). \quad (5)$$

The short coherence lengths and the anisotropic electronic properties of $\text{YBa}_2\text{Cu}_3\text{O}_{7-x}$ make it difficult to determine whether Eq. (4) or Eq. (5) should be used to describe σ' . The dimensionality of the fluctuations in $\text{YBa}_2\text{Cu}_3\text{O}_{7-x}$ depends upon the magnitude of the c -direction coherence length

$$\xi_c(T) = \xi_c(0) \epsilon_l^{-1/2} \quad (6)$$

in relation to the relevant layer thickness d . At high values of ϵ_l , where $\xi_c(T) < d$, the paraconductivity should manifest a two-dimensional nature. At low values of ϵ_l , near T_c^{MF} , $\xi_c(T)$ is expected to be greater than d , and the three-dimensional nature of the paraconductivity should be apparent. We attempted to fit both equations to the data.

1. Fit to the 2D AL model

The data were fit to the 2D AL form using a strategy employed by Hagen *et al.*⁸ They pointed out that if the

TABLE I. Aslamazov-Larkin 2D fit parameters.

| Fit | Range (K) | a ($\mu\Omega$ cm/K) | b ($\mu\Omega$ cm) | d (\AA) | T_c^{MF} (K) | χ^2 |
|------|-----------|-------------------------|-----------------------|----------------------|-----------------------|----------|
| AL2a | 96.0–200 | 0.760 | 11.1 | 2.82 | 87.41 | 1.0 |
| AL2b | 94.0–200 | 0.773 | 4.93 | 4.93 | 90.03 | 30.0 |
| AL2c | 93.7–200 | 0.788 | −1.39 | 6.64 | 90.93 | 62.5 |
| AL2d | 96.0–200 | 0.782 | 0.387 | 5.85 ^a | 90.66 | 31.8 |
| AL2e | 96.0–200 | 0.807 | −6.93 | 11.7 ^a | 92.75 | 122.0 |

^a Parameter was not varied in the fit.

paraconductivity in $\text{YBa}_2\text{Cu}_3\text{O}_{7-x}$ is two dimensional in nature, and if it follows the AL theory, the temperature dependence of both σ_n and σ' is the same (T^{-1}). Any attempt to fit the high-temperature resistivity data by an extrapolation method in the way it was done for polycrystalline samples²⁻⁴ will underestimate σ' and cause it to fall rapidly to zero at high ϵ_l . To avoid this problem, Hagen *et al.* used an equation similar to this (but did not replace ϵ by ϵ_l) to fit the conductivity data over a range $T_c + 1 < T < 260$ K, and they treated a and b as adjustable parameters

$$\sigma = \sigma_n + \sigma' = \frac{1}{aT+b} + \frac{e^2}{16\hbar d} \epsilon_l^{-1}. \quad (7)$$

In Eq. (7), two additional adjustable parameters appear: d is the thickness of the two-dimensional layer, and T_c^{MF} is the mean-field transition temperature. Following this procedure we find the results shown in Table I. We obtained the best fit for a temperature range $96 < T < 200$ K; it is labeled AL2a in Fig. 5. (Note that T_c^{MF} is one of the adjustable parameters, and that it is involved in the definition of ϵ_l in Fig. 5 and some of the later figures, so each fit produces a different set of data points.) The value $d=2.8$ Å and $T_c^{\text{MF}}=87.4$ K were extracted from this fit, which extends over a range in ϵ_l of 0.09 to 0.8. Fixing $d=5.85$ and 11.7 Å (0.5 and 1.0 times the unit-cell size, respectively) in fits AL2d and AL2e increased the value of T_c^{MF} , moving it closer to T_c , but resulted in much lower-quality fits, with χ^2 increasing by a factor of 122. As the fit range was chosen to be closer to T_c , the value of T_c^{MF} increased, moving closer to T_c , the value of d also increased to $d=6.6$ Å, and χ^2 increased by a factor of 62 from the fit AL2a, as shown for AL2b and AL2c in Table

I and Fig. 5. The value $d=2.8$ Å found for the best fit AL2a is about the same as the distance between copper oxide planes,²⁰ and is approximately one-quarter of the unit-cell size of 11.7 Å.

Hagen *et al.* found values of d ranging from 5.7 to 30 Å, with T_c^{MF} ranging from 3 to 5 K below T_c . The value of d is not given by theory. Oh *et al.*⁶ used $d=11.7$ Å; Hagen *et al.* used 5.85 Å. Our results indicate a smaller value for d , 2.8 Å, which is still consistent with the crystal structure. The paraconductivity for the AL2a fit rises too rapidly for any reasonable power law below $\epsilon_l=0.09$ and appears to show no evidence of three-dimensional fluctuations (a slope of $-\frac{1}{2}$) near T_c . Our value of T_c^{MF} is 5.6 K below T_c . These results are similar to those of Hagen *et al.*, who suggested that T_c^{MF} is several degrees below T_c because the critical region may be entered before the crossover to three-dimensional superconductivity occurs.

2. Fit to the 3D AL model

An attempt was made to fit the data to the 3D AL form using the method employed by us to fit paraconductivity data for polycrystalline samples.³ In this method, the linear portion of the high-temperature resistivity data was fit to $\rho=aT+b$. This fit was extrapolated down to T_c and the paraconductivity near T_c defined as $\sigma'=\sigma_n-1/(aT+b)$. The resulting fit, shown in Fig. 6, was qualitatively similar to our previous ones.³ The fit extended over the range $0.006 < \epsilon_l < 0.05$, with the paraconductivity rapidly falling to zero above $\epsilon_l=0.05$. The three-dimensional coherence length (averaged in some way over crystal directions) obtained from this fit was $\xi(0)=1.1$ Å,

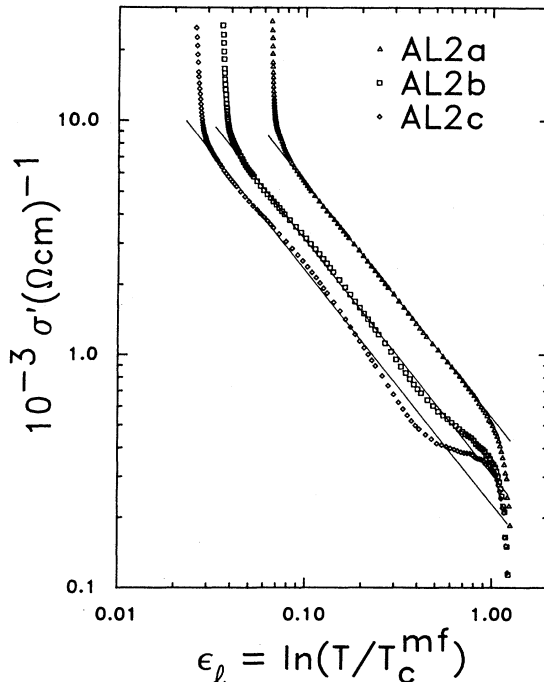


FIG. 5. σ' vs ϵ_l for three 2D AL fits listed in Table I.

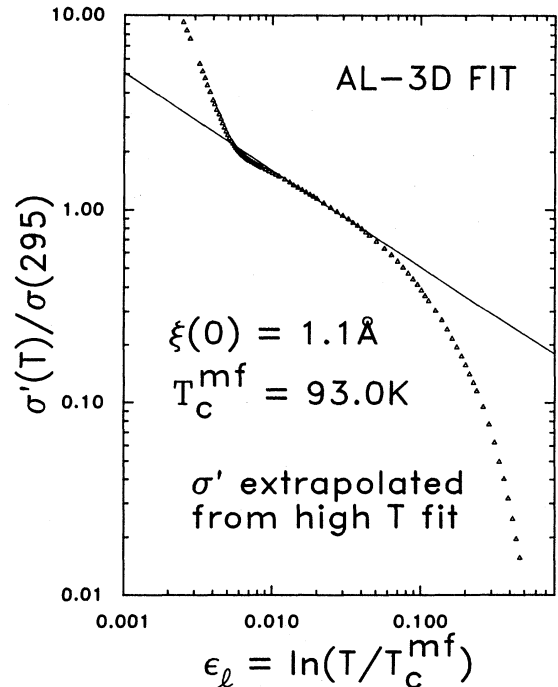


FIG. 6. σ' vs ϵ_l for the 3D AL extrapolation fit.

which is significantly smaller than the value 13–22 Å found for the polycrystalline samples, and is also nonphysically small for a 3D model.

An attempt was made to fit the 3D AL model by a better method. Equation (8) was employed, using the same strategy as in the 2D AL case

$$\sigma = \sigma_n + \sigma' = \frac{1}{aT+b} + \frac{e^2}{32\hbar\xi(0)} \epsilon_l^{-1/2}. \quad (8)$$

The resultant fit parameters are shown in Table II, and three of the fits are plotted in Fig. 7. The best fit over an extended temperature range AL3a occurred for $96.0 < T < 200$ K as in the 2D AL case. The values $\xi(0) = 0.46$ Å and $T_c^{MF} = 91.0$ K were extracted from this fit. The values of T_c^{MF} and $\xi(0)$ increased as the fit range was moved closer to T_c , with an increase in χ^2 to 22, as seen in AL3b and AL3c. The a parameter, representing the slope of the normal-state resistivity, is approximately 30% larger than the slope of the data, giving an excessively large fluctuation contribution to the total conductivity. Attempts to fit the data over a limited temperature range near T_c (AL3e, AL3f, and AL3g) present the same problem. The small three-dimensional coherence length $\xi(0) < 1.0$ Å is inconsistent with a three-dimensional picture, and the poor quality of the fits indicate that the 3D AL model does not account for the data.

D. Fit to the LD model

The Lawrence-Doniach expression for the paraconductivity is

$$\sigma' = \frac{e^2}{16\hbar d \epsilon_l} \{1 + [2\xi_c(0)/d]^2 \epsilon_l^{-1}\}^{-1/2}. \quad (9)$$

This expression is derived for layered superconductors, and may be applicable to $\text{YBa}_2\text{Cu}_3\text{O}_{7-x}$, with its layered atomic structure. Equation (9) reduces to the 2D AL result for large ϵ_l when $\xi_c(0)$ is less than the layer spacing d . Near T_c , for small values of ϵ_l , $\xi_c(T)$ may be greater than d ; in this case, the LD expression reduces to the 3D AL result.

The crossover from two- to three-dimensional fluctuations occurs at a temperature T_0 , defined by setting $\xi_c(T_0)$ equal to half the unit-cell size of 11.7 Å (or half the distance between Cu-O planes), the former yielding

$$T_0 = T_c^{MF} = \exp\{[\xi_c(0)/5.85 \text{ Å}]^2\}. \quad (10)$$

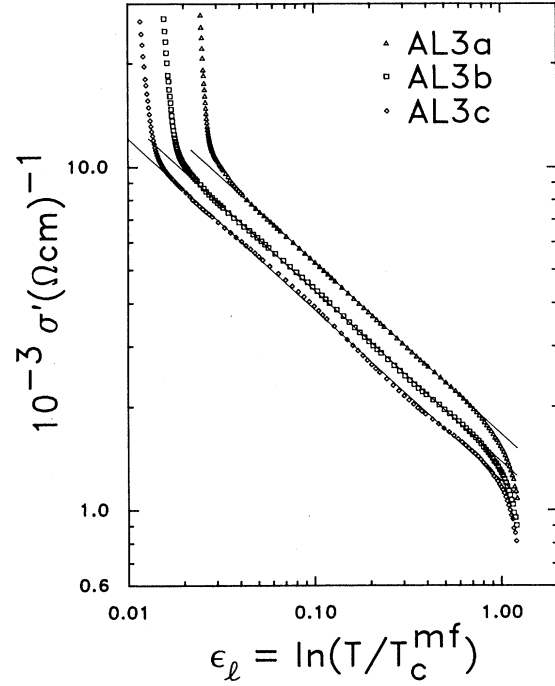


FIG. 7. σ' vs ϵ_l for three 3D AL fits listed in Table II.

Our inability to find reasonable fit parameters for the 3D AL model near T_c indicates that it should be difficult to find good fits to the LD model there, since the LD model predicts a two- to three-dimensional crossover near T_c .

Equation (11) was used with five adjustable parameters to fit the data:

$$\sigma = \sigma_n + \sigma' = \frac{1}{aT+b} + \frac{e^2}{16\hbar d \epsilon_l} \{1 + [2\xi_c(0)/d]^2 \epsilon_l^{-1}\}^{-1/2}. \quad (11)$$

The fit parameters are collected in Table III. The fits differ in the temperature range over which the data were fit and the variables which were held constant during the fit. The best fits were found over a temperature range $96 < T < 200$ K, and the quality of fit deteriorated as the lower end of the fitting range was decreased toward T_c , as in the AL fits. The fits LDa, LDb, and LDc are plotted in

TABLE II. Aslamazov-Larkin 3D fit parameters.

| Fit | Range (K) | a ($\mu\Omega$ cm/K) | b ($\mu\Omega$ cm) | $\xi(0)$ Å | T_c^{MF} (K) | χ^2 |
|------|-----------|-------------------------|-----------------------|------------|--------------------|----------|
| AL3a | 96.0–200 | 1.03 | −3.38 | 0.457 | 91.02 | 1.40 |
| AL3b | 94.0–200 | 0.981 | −4.51 | 0.552 | 91.85 | 10.7 |
| AL3c | 93.7–200 | 0.960 | −6.13 | 0.627 | 92.22 | 22.0 |
| AL3d | 96.0–200 | 0.931 | −6.00 | 0.725 | 93.00 ^a | 27.8 |
| AL3e | 93.5–98.5 | 0.724 ^a | 2.84 ^a | 1.14 | 93.00 ^a | 116.0 |
| AL3f | 93.5–98.5 | 1.15 | −40.1 | 1.24 | 93.00 ^a | 93.9 |
| AL3g | 93.7–98.5 | 1.68 | −93.4 | 1.45 | 93.00 ^a | 2.54 |

^a Parameter was not varied in the fit.

TABLE III. Lawrence-Doniach fit parameters.

| Fit | Range (K) | a ($\mu\Omega$ cm/K) | b ($\mu\Omega$ cm) | d (\AA) | ξ_c (\AA) | T_c^{MF} (K) | T_0 (K) | ξ^2 |
|-----|-----------|-------------------------|-----------------------|----------------------|--------------------------|-----------------------|-----------|---------|
| LDa | 96.0–200 | 0.790 | 13.9 | 1.71 | 0.435 | 90.55 | 91.05 | 0.500 |
| LDb | 94.0–200 | 0.823 | 7.98 | 1.58 | 0.553 | 91.80 | 92.62 | 13.1 |
| LDc | 93.7–200 | 0.813 | 4.70 | 2.13 | 0.645 | 92.22 | 93.34 | 25.8 |
| LDd | 96.0–200 | 0.782 | 0.383 | 5.85 ^a | 0.075 | 90.69 | 90.70 | 32.6 |
| LDe | 96.0–200 | 0.804 | 3.18 | 2.67 | 0.749 | 93.00 ^a | 94.53 | 32.7 |
| LDf | 96.0–200 | 0.819 | –8.80 | 11.7 ^a | 1.5 ^a | 94.56 | 100.8 | 175.0 |

^aParameter was not varied in the fit.

Fig. 8. These three fits differ in the temperature range over which the data were fit. The quality of the fits was better than the 2D AL fits over the corresponding temperature ranges. This is not surprising, since the LD model has five adjustable parameters, while the 2D AL model has four. The value $d=1.71$ \AA obtained from the best fit LDa is smaller than the value of $d=2.82$ \AA found above in the 2D AL fits. The value of $\xi_c(0)$ from the best LD fit is 0.44 \AA . This value seems surprisingly small. It is not actually known, however, that ξ_c approaches 0.44 \AA as T becomes much less than T_c , since we do not know the temperature dependence of ξ_c with any certainty in the high-temperature superconductors. The values of T_c^{MF} lie 1 to 3 K below T_c . It is surprising to find $T_c^{\text{MF}} < T_c$, although this was also found by Hagen *et al.*⁸ Conclusions should probably not be drawn from any of our data taken below 93.6 K, where the data fit none of the theories.

In the work of Oh *et al.*, T_c^{MF} was determined by extrapolating the linear region near T_c of a plot of σ'^{-2} vs T to $\sigma'^{-2}=0$. They found values of T_c^{MF} to be 1–2 K above

the zero-point resistance temperature T_c . They introduced an additional parameter C into Eq. (11), substituting $Ce^2/16\hbar d\epsilon$ for $e^2/16\hbar d\epsilon$. They were forced to do this because of their assumption that $d=11.7$ \AA , the unit-cell size. The values of C they extracted from their fits ranged from 3.3 to 7.4 \AA , and 1.5 $\text{\AA} < \xi_c(0) < 2.0$ \AA . A fit with $C \neq 1$ and a given value of d is exactly the same as a fit with $C=1$ and a smaller value of d , with the same ratio of $\xi_c(0)$ to d .

Figure 9 is a plot of σ'^{-2} vs T , using the a and b parameters of fit LDa to define σ' . An intercept of 91.7 K is found by extrapolating the linear part of this plot near T_c ($96 < T < 100$ K) to $\sigma'^{-2}=0$ (the dotted line of Fig. 9). The intercept of the curve is 1.1 K above the mean-field transition temperature predicted from the nonlinear fit. The curve obtained from the nonlinear fit to LDa is plotted as the dashed line in Fig. 9 for comparison. The two procedures give a different value for T_c^{MF} because σ'^{-2} is quadratic in T in the LD model, and the linear extrapolation near T_c is not good enough to accurately predict

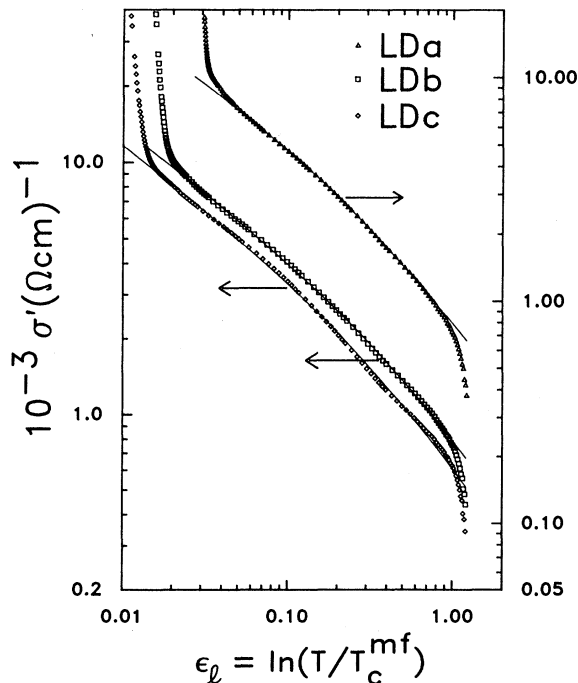


FIG. 8. σ' vs ϵ_l for three LD fits listed in Table III.

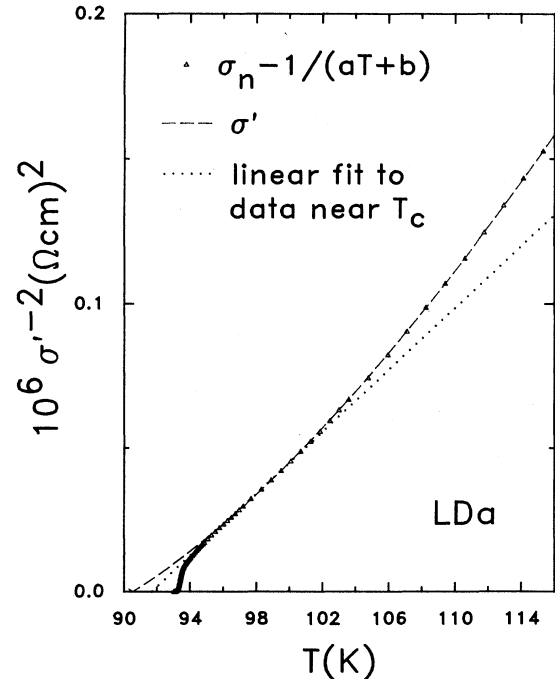


FIG. 9. σ'^{-2} vs T plot of the LDa fit listed in Table III.

T_c^{MF} . Similar plots were found for several of the other fits listed in Table III.

Hagen *et al.* conclude that the LD equation does not fit their data. In defining σ' for the LD fits, they used σ_n as that found from their AL fits, and chose T_c at the value where $1/\sigma'$ extrapolates to zero, rather than allowing it to vary freely. We find that allowing σ_n and T_c^{MF} to vary results in good fits to the data.

It appears possible to fit the data well with the LD model. The fit is good over a wider range in ϵ_l values ($0.05 < \epsilon_l < 0.8$) than the 2D AL fits and has a lower χ^2 value than either the 2D AL or 3D AL fits. This seems surprising at first, in light of our inability to get reasonable fits to the 3D AL model. Further thought resolves the paradox: The crossover temperature T_0 from 3D to 2D behavior as given by Eq. (10), using the values of T_c^{MF} and $\xi_c(0)$ from the LDa fit, is $T_0 = 91.1$ K which is 1.9 K below T_c . The slope of the LDa fit in Fig. 8 at high ϵ_l is close to -1 , indicating 2D behavior, as it should. Near $\epsilon_l = 0.05$, where the LDa fit diverges from the data, the slope is -0.76 , indicating the transition to 3D behavior has begun, but the superconducting transition is reached before it can be completed.

E. Fit to the MT model

Maki and Thompson reformulated the AL theory by reconsidering the role of the decay of the superconducting pairs into quasiparticles, and vice versa. In the presence of weak pair-breaking effects, newly formed quasiparticles may continue in a state of nearly equal and opposite momenta until they recombine to form fluctuation pairs. The enhancement in the conductivity contributed by this process is limited by strong inelastic scatterers and by the presence of pair-breaking interactions, such as that contributed by magnetic impurities. Maki and Thompson's work added an additional term to the AL result. The resulting theory should probably be called the Aslamazov-Larkin-Maki-Thompson (ALMT) model, but we refer to it as the Maki-Thompson (MT) model for brevity. The two-dimensional MT result is as follows:

$$\sigma' = \sigma_{\text{AL}} + \sigma_{\text{MT}}, \quad (12)$$

$$\sigma' = \frac{e^2}{16\hbar d} \epsilon_l^{-1} + \frac{e^2}{8\hbar d} \frac{1}{\epsilon_l - \delta} \ln(\epsilon_l/\delta). \quad (13)$$

In this equation δ represents the reduced temperature shift $\delta = (T_{c0} - T_c)/T_c$ induced by pair-breaking interactions.

We fit the data to the following five-parameter nonlinear equation:

$$\sigma' = \frac{1}{aT+b} + \frac{e^2}{16\hbar d} \epsilon_l^{-1} + \frac{e^2}{8\hbar d} \frac{1}{\epsilon_l - \delta} \ln(\epsilon_l/\delta). \quad (14)$$

The parameters obtained from fits to the data are shown in Table IV. The fits differ in the temperature range over which the data were fit and the variables which were held constant during the fit. As for the other three models, the best fits to the data occurred for a temperature range $96 < T < 200$ K, with the quality of the fit decreasing as the lower end of the fitting region was lowered toward T_c . This can be seen in fits MTa, MTb, and MTc of Table IV, which are plotted in Fig. 10. The quality of the fits is similar to that of the 2D AL and LD models over the corresponding temperature ranges.

The fitting procedure for the MT case was not able to uniquely determine values for d and δ ; Table IV contains fits of near equal quality with values for d and δ ranging from $11.7 < d < 60$ Å and $4.39 \times 10^{-2} > \delta > 8.01 \times 10^{-6}$. (In clean aluminum films,²¹ by comparison, the parameter δ is about 10^{-4} .) A broad minimum in χ^2 occurs for this range of values. Our inability to uniquely determine a , b , and T_c^{MF} in the MT case is the cause of this problem. The data can be fit with the MT model, but we cannot draw any conclusions as to the validity of this model in describing the data, since the parameters are not well determined.

IV. SUMMARY AND CONCLUSIONS

Our analysis rests on the assumption that the normal-state conductivity is a linear function of temperature. This seems reasonable because of the extremely linear temperature dependence of the sample's conductivity between 150 and 240 K.

Using the two-dimensional AL theory the best value of d is 2.8 Å. The best value of $\xi(0)$ is 0.46 Å for the three-dimensional AL fits, which should be some average of ξ_a , ξ_b , and ξ_c ; this value of $\xi(0)$ is, therefore, too small for a

TABLE IV. Maki-Thompson fit parameters.

| Fit | Range (K) | a ($\mu\Omega$ cm/K) | b ($\mu\Omega$ cm) | d (Å) | δ | T_c^{MF} (K) | T_{c0} (K) | χ^2 |
|--------|-----------|-------------------------|-----------------------|-------------------|-----------------------|-----------------------|--------------|----------|
| MTa | 96.0–200 | 0.815 | 10.7 | 16.9 | 1.42×10^{-2} | 89.50 | 94.32 | 0.638 |
| MTb | 94.0–200 | 0.833 | 3.98 | 13.5 | 7.30×10^{-2} | 91.15 | 99.79 | 17.6 |
| MTc | 93.7–200 | 0.832 | 0.567 | 17.6 | 5.86×10^{-2} | 91.72 | 98.45 | 36.2 |
| MTd | 96.0–200 | 0.837 | 10.2 | 11.7 ^a | 4.40×10^{-2} | 89.67 | 97.09 | 0.597 |
| MTe | 96.0–200 | 0.807 | 10.8 | 20.0 ^a | 7.81×10^{-3} | 89.33 | 93.73 | 0.652 |
| MTf | 96.0–200 | 0.792 | 10.9 | 30.0 ^a | 1.22×10^{-3} | 88.81 | 93.11 | 0.733 |
| MTg | 96.0–200 | 0.784 | 11.0 | 40.0 ^a | 2.02×10^{-4} | 88.44 | 93.02 | 0.789 |
| MT h | 96.0–200 | 0.780 | 10.5 | 50.0 ^a | 4.24×10^{-5} | 88.37 | 93.00 | 0.873 |
| MTi | 96.0–200 | 0.777 | 10.4 | 60.0 ^a | 8.01×10^{-6} | 88.2 | 93.00 | 0.919 |
| MTj | 96.0–200 | 0.772 | 10.2 | 70.0 ^a | 2.18×10^{-6} | 88.40 | 93.00 | 1.40 |

^aParameter was not varied in the fit.

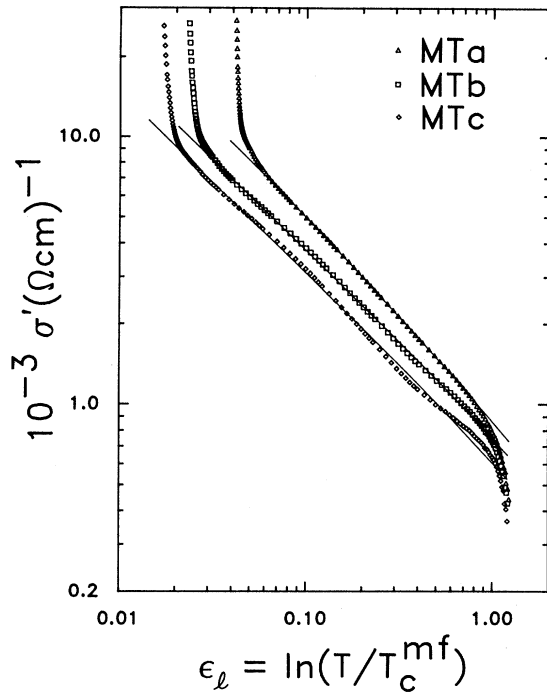


FIG. 10. σ' vs ϵ_l for three MT fits listed in Table IV.

three-dimensional theory. In the MT case, the fitting procedure does not give well-defined fitting parameters.

Although good fits to the data are obtained for all four theories, the Lawrence-Doniach theory provides a better fit (with one more adjustable parameter) over a wider range in ϵ_l than the Aslamazov-Larkin theory does in either 2D or 3D. The best fit to the LD theory provides the parameters $d=1.71$ Å and $\xi_c(0)=0.44$ Å. A $\xi_c(0)$ as small as that raises theoretical problems. The number of Cooper pairs in a region of diameter $\xi_{a,b}(0)$ and thickness $\xi_c(0)$ would be less than unity. Near T_c , however, the coherence length would be larger, and this problem would be alleviated.

We find it surprising that the LD theory fits our data for such a wide range of ϵ_l values, up to a temperature of 2.2 times T_c^{MF} . For all four theories, T_c^{MF} is (surprisingly) less than the zero-resistance temperature T_c by several K, with the paraconductivity deviating from the theories with decreasing T near $T_c+0.6$ K. This rapid increase in the paraconductivity near T_c may point to some deficiency in the theories in describing the data, but, as we have suggested³ previously, it may simply show that the region between T_c and $T_c+0.6$ K is the critical region, where the fluctuations in the number of superconducting electrons is not smaller than its average value. Another possible explanation is that below $T_c+0.6$ K, inhomogeneities in the sample have an observable effect. Most people who have worked carefully with $\text{YBa}_2\text{Cu}_3\text{O}_{7-x}$ have come to realize that the samples are not perfectly homogeneous. The structure near the peak of the $d\rho/dT$ curve in Fig. 3 is an indication of such inhomogeneity. Perhaps there is a range of transition temperatures in the sample, δT_c . Figure 3 would indicate that δT_c may be on the order of 0.2 K.

Then none of the theories can be expected to fit within roughly δT_c of the apparent T_c . It should be noted that when T lies in the range $T_c+0.2$ K to $T_c+0.6$ K, $\xi_c(0)/[\ln(T/T_c^{MF})]^{1/2}$ is approximately 2.5 Å, so inhomogeneities of all scales, down to atomic dimensions, would be expected to influence the superconducting properties. For temperatures far above T_c , the effects of inhomogeneities could average out.

Our results agree well with those of Oh *et al.* In comparing their results with the theory of Lawrence and Doniach, however, they assumed that $d=11.7$ Å, the size of the unit cell. This assumption forced them to introduce an adjustable parameter C . There is no reason, however, why d should not be approximately the spacing between Cu-O planes, as we have found. Oh *et al.* pointed out that their experiment determined $2\xi_c(0)/d$ more unambiguously than d , and their result $2\xi_c(0)/d=0.3$ is smaller than ours, 0.54. If the fit is done using ϵ instead of ϵ_l , as they did, we get $d=2.47$ Å and $\xi_c(0)=0.43$ Å, so $2\xi_c(0)/d=0.35$ in agreement with the data of Oh *et al.*

The crossover to 3D fluctuations found by Oh *et al.* was at a temperature T_0 above T_c with $T_0/T_c^{MF}=1.1$. We get a value of T_0 below T_c , but slightly above T_c^{MF} , with $T_0/T_c^{MF}=1.01$. With our value of T_0 we still find the slope tending toward $-\frac{1}{2}$ indicating 3D behavior before the superconducting transition, in disagreement with Hagen *et al.*, so we can fit the data to the LD theory. Fitting the data to the 2D AL theory in a similar manner as Hagen *et al.*, we find that the transition to 3D behavior is cutoff before completion by what we believe are critical fluctuations near T_c or the effects of sample inhomogeneities at a scale of a few Å.

From our LD fits, we find the crossover temperature, $T_0=90.7$ K to be less than T_c , but from the beginning of a change in slope of the best fit (LDa) near T_c , behavior tending toward 3D fluctuations is evident. Our value of T_0 is consistent with our inability to fit the 3D AL model with reasonable fit parameters near T_c . It is also consistent with our reasonably good 2D AL fits near T_c . The value of $\xi_c(T)$ from the best LD fit is less than half the unit-cell size near T_c , accounting for 2D behavior there.

Larger values of $\xi_c(0)$ than ours, obtained from resistive measurements of $H_{c2}(T)$, have recently been called into question by the discovery of flux-lattice melting.^{22,23} The many resistance measurements of $H_{c2}(T)$ indicate the field at which the flux lattice melts, rather than the field at which the material is forced into the normal state. It appears that a $\xi_c(0)$ result closer to ours would be indicated by Lee, Klemm, and Johnston measurements of fluctuation diamagnetism;²⁴ they find $\xi_c(0)=1.4 \pm 0.2$ Å. [It is not possible to estimate the coherence length from measured values of $H_{c1}(0)$, because published values range from 1 to 5000 Oe.]

ACKNOWLEDGMENTS

Support for this work was provided in part by National Science Foundation Grant No. NSF DMR 87-14555. We are grateful to Nigel Goldenfeld and Elihu Abrahams for alerting us to the necessity of replacing ϵ by ϵ_l in the usual paraconductivity equations. C. C. Tsuei helped us improve the manuscript.

- ¹J. S. Shier and D. M. Ginsberg, *Phys. Rev.* **147**, 384 (1966).
- ²P. P. Freitas, C. C. Tsuei, and T. S. Plaskett, *Phys. Rev. B* **36**, 833 (1987).
- ³N. Goldenfeld, P. D. Olmsted, T. A. Friedmann, and D. M. Ginsberg, *Solid State Commun.* **65**, 465 (1988).
- ⁴M. A. Dubson, J. J. Calabrese, S. T. Herbert, D. C. Harris, B. R. Patton, and J. C. Garland, in *Novel Superconductivity*, edited by S. A. Wolf and V. Z. Kresin (Plenum, New York, 1987), p. 981.
- ⁵L. G. Aslamazov and A. I. Larkin, *Fiz. Tverd. Tela* **10**, 1104 (1968) [*Sov. Phys. Solid State* **10**, 875 (1968)].
- ⁶B. Oh, K. Char, A. D. Kent, M. Naito, M. R. Beasley, T. H. Geballe, R. H. Hammond, A. Kapitulnik, and J. M. Graybeal, *Phys. Rev. B* **37**, 7861 (1988).
- ⁷W. E. Lawrence and S. Doniach, *Proceedings of the Twelfth International Conference on Low-Temperature Physics, Kyoto, 1970*, edited by E. Kanda (Keigaku, Tokyo, 1970), p. 361.
- ⁸S. J. Hagen, Z. Z. Wang, and N. P. Ong (unpublished).
- ⁹K. Maki, *Prog. Theor. Phys.* **39**, 897 (1968); **40**, 193 (1968).
- ¹⁰R. S. Thompson, *Phys. Rev. B* **1**, 327 (1970).
- ¹¹J. P. Rice, B. G. Pazol, D. M. Ginsberg, T. J. Moran, and M. B. Weissman, *J. Low Temp. Phys.* **72**, 345 (1988).
- ¹²L. J. van der Pauw, *Philips Res. Rep.* **16**, 187 (1961).
- ¹³J. R. Matey, S. B. Dierker, and A. C. Anderson, *Rev. Sci. Instrum.* **50**, 671 (1979).
- ¹⁴R. Micnas, J. Ranninger, and S. Robaszkiewicz, *Phys. Rev. B* **36**, 4051 (1987).
- ¹⁵D. C. Johnston, S. K. Sinha, A. J. Jacobson, and J. M. Newsam, *Physica C* **153-155**, 572 (1988).
- ¹⁶K. Fosshem, O. M. Nes, T. Laegreid, C. N. W. Darlington, D. A. O'Connor, and C. E. Gough (unpublished).
- ¹⁷W. H. Press, B. P. Flannery, S. A. Teukolsky, and W. T. Vetterling, in *Numerical Recipes* (Cambridge Univ. Press, Cambridge, 1986), p. 523.
- ¹⁸L. P. Gorkov, *Zh. Eksp. Teor. Fiz.* **36**, 1918 (1959) [*Soviet Phys. JETP* **9**, 1364 (1959)].
- ¹⁹A. Corana, M. Marchesi, C. Martini, and S. Ridella, *ACM Trans. Math. Software* **13**, 262 (1987).
- ²⁰M. A. Beno. L. Soderholm, D. W. Capone II, D. G. Hinks, J. D. Jorgensen, J. D. Grace, Ivan K. Schuller, C. U. Segre, and K. Zhang, *Appl. Phys. Lett.* **51**, 57 (1987).
- ²¹G. A. Thomas and R. D. Parks, *Phys. Rev. Lett.* **27**, 1276 (1971).
- ²²Y. Yeshurun and A. P. Malozemoff, *Phys. Rev. Lett.* **60**, 2202 (1988).
- ²³P. L. Gammel, L. F. Schneemeyer, J. V. Waszczak, and D. J. Bishop, *Phys. Rev. Lett.* **61**, 1666 (1988).
- ²⁴W. C. Lee, R. A. Klemm, and D. C. Johnston (unpublished).